Journal of Hazardous Materials 209–210 (2012) 59–66

Contents lists available at SciVerse ScienceDirect

Journal of Hazardous Materials

journal homepage: www.elsevier.com/locate/jhazmat

Complexion between mercury and humic substances from different landfill stabilization processes and its implication for the environment

Chai Xiaoli*, Liu Guixiang, Zhao Xin, Hao Yongxia, Zhao Youcai

The State Key Laboratory of Pollution Control and Resource Reuse, Tongji University, Shanghai, 200092, China

ARTICLE INFO

Article history:
Received 1 September 2011
Received in revised form
22 December 2011
Accepted 25 December 2011
Available online 10 January 2012

Keywords:
Humic substances
Mercury
Landfill stabilization processes
EEM

ABSTRACT

Three-dimensional excitation emission matrix (EEM) fluorescence spectroscopy was employed to investigate the structural properties and Hg(II)-binding behavior of humic substances (HS) extracted from different landfill stabilization processes. The EEM fluorescence properties of humic acid (HA) are characterized by intense fluorescence at Ex/Em = 440/500 nm and Ex/Em = 380/460 nm. Two relatively strong fluorescence peaks appeared in the region of Ex/Em = 260–290/350–370 nm with the landfill time extended, which represented a protein-like or soluble microbial byproduct structure. The fluorescence EEM spectrum of fulvic acid (FA) featured a prominent peak of strong relative fluorescence intensity (FI = 1598) at Ex/Em = 330/440 nm (peak C) accompanied by a weak fluorophore (FI = 594) located at Ex/Em = 275/445 nm (peak D). There were strong interactions between HA and Hg, and the overall stability constant of Hg(II)–HA was mainly determined by the abundant O-ligands existing in HA. FA had a much higher Hg(II)-complexing capacity compared to HA samples, which may be ascribed to its relatively high content of carboxylic groups. The Hg(II)-complexing capacity of HA tended to decrease with stabilization process extension. The much higher Hg(II)-complexing capacity of FA than that of HA implied that FA played an important role in binding Hg(II) in early landfill stabilization process.

1. Introduction

With the rapid economic development in China, more and more mercury (Hg) and Hg-bearing solid waste are produced from household products, such as fluorescent lights, batteries, and thermometers. Due to the unseparated solid waste collection system widely adopted in China, a large amount of Hg-bearing solid waste is collected and disposed of in landfills. Many papers have reported that Hg is released from large-scale landfills into the air, soil, and underground water, making it a potential environmental risk for the future [1–7].

Mercuric species form complexes with natural dissolved organic matter (DOM) and especially its humified fraction called humic substance (HS) which is mainly composed of humic acid (HA) and fulvic acid (FA). This binding is known to affect the chemical and biological transformation and cycling of Hg in the environments [8–11]. DOM interacts significantly with both Hg and dimethylmercury, as seen in the close correlation between concentrations of Hg and DOM commonly found in aquatic environments [12,13].

The anoxic conditions of aquatic environments may increase the methylation of inorganic Hg [14] because the highly toxic methyl Hg compound is formed when anaerobic bacteria degrade organic substances. In contrast to the dominant role assigned to biotic processes in methylation, a number of investigators have provided evidence of abiotic Hg methylation [15–17]. In addition, Hg(II) ions may also be reduced to elemental Hg by DOM as a result of the interaction of humic substances with Hg(II) ions. These results show that DOM significantly influences the Hg species transformation and biological uptake that leads to the accumulation of highly toxic methylmercury.

Although a large body of literature is now available on the interactions of Hg(II) with DOM in natural sediments and aquatic environments, the interaction of HS with Hg as well as its potential impacts on the species and fate of Hg have rarely been examined in different landfill stabilization processes.

Hg, as a paramagnetic metal, is able to quench the intrinsic fluorescence of HS ligands [18]. Monitoring the changes of fluorescence spectra of HS upon titration with Hg(II) can provide useful qualitative and quantitative information regarding the binding properties of HS–Hg(II). Previous studies have demonstrated that the fluorescence-quenching titration technique combined with various mathematical approaches introduced by former researchers can determine important parameters like the metal ion complexing capacities of HS and the stability constants of metal ion–HS complexes, both of which are essential for predicting the behavior and performance of metal ions in the environment [19–23].

* Corresponding author. Tel.: +86 21 65981831; fax: +86 21 65980041.
E-mail addresses: xlchai@mail.tongji.edu.cn, xlchai@tongji.edu.cn (X. Chai).

0304-3894/$ – see front matter © 2012 Elsevier B.V. All rights reserved.
doi:10.1016/j.jhazmat.2011.12.077

The objective of the present study was to investigate the binding behavior of HS with Hg in different landfill stabilization processes. The complexing capacities and stability constants of HS–Hg complexes were determined in order to examine the role of HS on the release and transfer of Hg from a landfill. Extended knowledge of Hg binding to HS in a landfill will be useful for predicting transport and fate of Hg and for facilitating the development of effective measures to prevent Hg from migrating and dispersing from landfills into the surrounding environment.

2. Materials and methods

2.1. Sample collection and preparation

All samples for this study were collected from the Shanghai Laogang Landfill (N31°03′13.4″, E121°53′52.9″), the largest landfill in China. This landfill was constructed in 1985 along the shore of the East China Sea and began operation at the end of 1989. It treats about 5000 tons of refuse daily, 75% of which is generated in the city of Shanghai. Refuse from different years is deposited in different units of the landfill, and the total refuse amount at the time of the study was about 30 million tons.

Refuse samples were collected on March 8, 2005. Landfill refuse from the years 1989, 1992, and 1996 was chosen as our original refuse samples. So they had been under the landfill for 16, 13, and 9 years, respectively. A systematic sampling plan was designed because solid waste is highly heterogeneous. First, surface vegetables and cover soil were removed manually, and refuse samples were collected at 1-m intervals from the surface to a maximum depth of 4 m. Refuse samples of at least 50 kg were collected at each depth. In each landfill cell, a total of 16 samples were collected from 4 sampling sites. The sampling areas were each approximately 2–3 m^2, depending on the section area of the dig. The refuse samples from each landfill cell were mixed and homogenized. After the samples were oven-dried at 50 °C, the basic physical composition of the samples was measured by weighing the components. Nondegradable matter such as stones, glass bottles, plastic film (bags), and rubber in the samples was removed, and the remains were sieved through a 10-mm mesh. The materials that passed through were then sieved through a 2-mm mesh to remove small-particle heterogeneous debris. The materials that passed through the 2-mm mesh were broken into small pieces by hammer, ball miller, or grinder, if necessary, and then resieved through a 0.25-mm mesh. The samples that passed through the 0.25-mm mesh were used to extract HA and FA.

2.2. Humic substances extraction procedure

Isolation and purification procedures were carried out according to the method recommended by the International Humic Substances Society. The extraction procedure is shown in Fig. 1. Briefly, a 100-g sample was extracted by 0.1 M HCl with the liquid/solid ratio (L/S) = 10 for 1 h. The residue was separated from the supernatant by centrifugation (4000 rpm, 20 min) and was subsequently neutralized to pH 7 using 1 M NaOH. One liter of 0.1 M NaOH was then added to the residue, and the suspension was shaken slowly under N_2 atmosphere for 4 h. The residue was removed from the dark-colored supernatant by centrifugation (4000 rpm, 20 min). The HA fraction was separated by acid precipitation (pH 1) with 6 M HCl, leaving the FA fraction in the supernatant. The precipitate was redissolved in a minimum of 0.1 M KOH/0.3 M KCl to remove mineral impurities using the mixture of 0.1 M HCl/0.3 M HF, then dialyzed against distilled water until Cl^- could not be detected. The FA fraction was purified by an adsorption resin (XAD-8, Supelco, Inc.), and the alkaline elution was passed through H^+-saturated cation exchange resin (AG-MP-50, Bio-Rad, Inc.). All the extractions were freeze-dried for further chemical analysis. The HA and FA extracted from the refuse sample that had been under landfill for 16, 13 and 9 years was named HA16, HA13, HA9 and FA13, respectively.

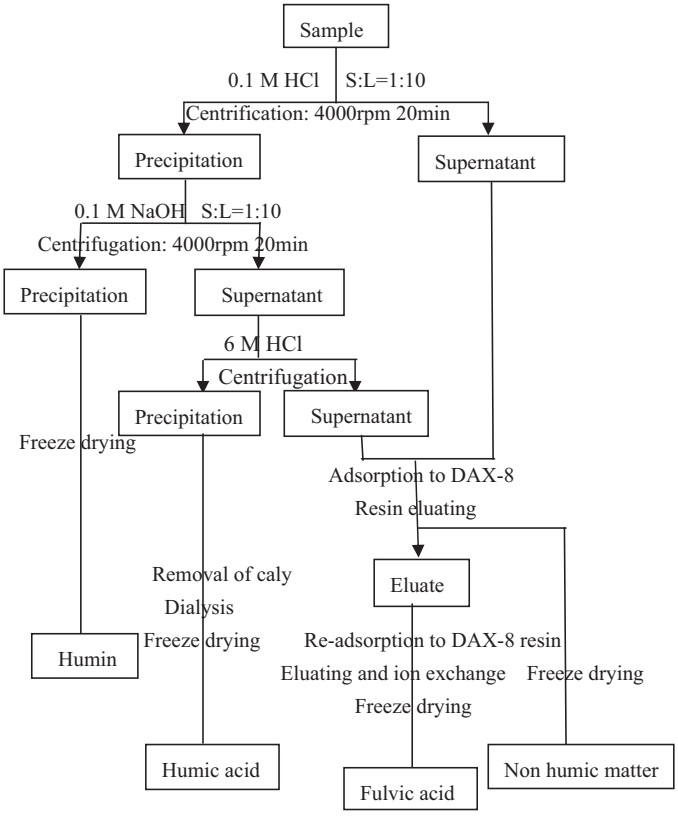

Fig. 1. The extraction and purification process of humic substances.

2.3. Fluorescence measurements

The 3DEEM fluorescence spectra were determined on a fluorescence spectrophotometer (F-4500, Hitachi, Japan) with a 150-W Xe arc lamp. The EEM spectra were collected with subsequent scanning of emission spectra from 300 to 550 nm at 5 nm increments by varying the excitation wavelength from 250 to 500 nm at 5 nm increments. The bandpass width was 5 nm for excitation and 10 nm for emission, and the scan speed was 2400 nm/min. The spectra were obtained by subtracting the spectra of Milli-Q water (18.2 MX cm, Millipore) as blank (recorded under the same conditions) to eliminate water Raman scatter peaks. Fluorescence emission intensities were expressed in arbitrary units and automatically corrected by the measurements for variations in excitation lamp spectral profiles and for any temporal intensity variations. The EEM plots were generated from fluorescence spectral data using Surfer 8.01 software.

2.3.1. Fluorescence quenching titration and data processing

Stock solutions of 50 mg/L HA and FA samples were prepared in 0.01 mol/L KNO_3. Two hundred milliliters of the stock solutions were titrated in 250-mL beakers with 0.01 M $Hg(NO_3)_2$ or 0.05 M $Hg(NO_3)_2$ solutions using an automatic syringe. pH was maintained at 6.00 and a constant stirring speed was provided using an automatic titrimeter (Titrando 842, Switzerland) with 0.1 M KOH and 0.1 M KNO_3. After each addition of titrant, the solution was allowed to fully react for 15 min at 18 °C under N_2 atmosphere prior to

fluorescence measurement. All chemicals used were AR grade, and Milli-Q water was used in all experiments.

The complexation parameters between Hg and landfill refuse HS were determined using the single-site fluorescence quenching model of Ryan and Weber [24]. This model assumes that metal ion binding occurs at identical and independent binding sites or ligands and that only 1:1 metal/ligand complexes are formed.

According to Ryan and Weber, the relationship between the fluorescence intensity (I) and the total metal ion concentration (C_M) is obtained through the following equation:

$$I = I_0 + (I_{ML} - I_0)\left(\frac{1}{2K_M C_L}\right)\left(1 + K_M C_L + K_M C_M - \sqrt{(1 + K_M C_L + K_M C_M)^2 - 4K_M^2 C_L C_M}\right)$$

In this, I_0 is the fluorescence intensity at the beginning of the titration (without adding metals); I_{ML} is the limiting value below which the fluorescence intensity does not change due to the addition of metal; and K_M and C_L are the conditional stability constant and total ligand concentration, respectively. By introducing the fluorescence intensity values determined experimentally at the various total metal ion concentrations used, the above equation can be solved by non-linear regression analysis for K, C_L, and I_{ML}. The optimum set of fitting parameters for each Hg–HS sample was obtained using the Quasi-Newton algorithm to minimize the sum of the squares of the differences between experimental and model-predicted values of I. The software SigmaPlot (SPSS) was used for the non-linear regression calculations.

2.3.2. Influence of the solution pH on the fluorescence properties

One hundred milliliters of each of the stock solutions were used to measure fluorescence in the presence and absence of 20 μmol/L Hg(II) at various pH. Using an automatic syringe, high concentrations of KOH and HNO_3 solution were added to adjust pH to the desired value to avoid the effects of concentration dilution.

3. Results and discussion

3.1. Chemical and structural characteristics of humic substances

The compositional, structural, and functional chemical properties of the landfill HSs studied in this work have been previously described [25]. Briefly, FA13 had a substantially higher content of O, a little more content of S and less content of C, N and H than all the HAs. FA13 was characterized by a relatively much higher content of carboxylic functional groups, *O*-alkyl C and polysaccharide-like components while HAs were found to have apparently more content of lignin and aromatic structures. As landfill time increased, the content of O, N and carboxylic functional groups decreased while the content of C, H, S and stable lignin and aromatic structures increased from HA9 to HA16. These demonstrated that the aromatic condensation, stability and humification degree of HA are much higher than that of FA and these degrees increased for HA as landfill time extended.

3.2. Fluorescence spectra of humic substances

EEM spectra of the HS measured in the absence and presence of Hg(II) at a total concentration of 30 μM are shown in Fig. 2. The fluorescence EEM spectrum of HA9 was characterized by two main fluorophores of peak A and peak B. Peak A was located at Ex/Em = 440/500 nm with a relatively high fluorescence intensity (FI) value of 238.9, and peak B was centered at Ex/Em = 380/460 nm with an FI value of 224.8. HA13 showed almost the same fluorescence EEM spectrum though the FI value was lower. Fluorescence peaks of peak A with longer wavelengths are associated with the presence of extended, linearly condensed aromatic ring networks and other unsaturated bonds that are capable of a great degree of conjugation with high molecular weight and humification degree. By contrast, fluorescence peak B with shorter wavelength may be ascribed to the presence of simple structural components of wide molecular heterogeneity, relatively small molecular weight, and a low degree of aromatic polycondensation, conjugated chromophores, and humification [26,27].

Quite different from that of HA9 and HA13, peak A was missing in the EEMs of HA16 whereas two relatively strong fluorescence peaks appeared in the region of Ex/Em = 260–290/350–370 nm, which represented a protein-like or soluble microbial byproduct structure [28].

The fluorescence EEM spectrum of FA13 featured a prominent peak of strong relative FI (1598) at Ex/Em = 330/440 nm (peak C) accompanied by a weak fluorophore located at Ex/Em = 275/445 nm (peak D) with an FI value of 594. Peak C was produced by structures containing phenolic groups, the aromatic structure with electron-donating substituents such as hydroxyl that induce a high, intense fluorescence of peak C. Peak D probably represented chromophores with high carboxylic functional groups that can reduce fluorescence intensity as an electron-withdrawing substituent. This is consistent with the results of our previous study, in which we found that FA contains as much as 20% carboxylic carbon [25]. Furthermore, the shorter excitation wavelength position of chromophores with high carboxylic functional groups than those containing phenolic groups has also been previously confirmed [27].

Peaks A and B were both at longer wavelengths than peaks C and D, which indicated higher molecular weight and aromatic polycondensation degrees of HAs compared to those of FAs. The relatively stronger fluorescence intensity of HA9 than that of HA13 demonstrated its lower aromatic and humification degrees due to less landfill time [26,29]. The aromatic condensation and humification degrees of HA increased with the landfill time and thereby led to the larger molecular weight components of HA, which increased its ability to physically encapsulate proteinaceous material into its complicated structure. On the other hand, the proteinaceous material produced from the degradation of organic substances further reacted with the humified centers of HA through chemical bonding with the extended landfill time. These two interactions brought about the unique fluorescence characteristics of HA16.

A marked decrease of fluorescence intensity was observed for all of the HS samples with the addition of Hg(II), which indicated that there was a strong, complex reaction between Hg and the fluorescence functions of HS. No shift of fluorescence peaks was observed for HA16 or HA13. However, peak A of HA9 showed a slight red-shift, and peak B showed an apparent blue-shift upon addition of Hg(II). In addition, the fluorescence intensity of HA9 was found to be quenched in the largest scale. These findings indicate that HA9 may be under a greater modification of electronic structure upon interaction with Hg(II). The different resultant changes of the fluorescence EEM spectra of the HA samples upon interaction with Hg(II) demonstrated the different interaction modes and strength of the achieved bonding of Hg(II) to HA, which depends on the conformational and functional chemical properties and the humification degree of HA.

3.3. Hg(II)-ion binding parameters of HS

As shown in Fig. 3 , a successive decrease of fluorescence intensity of both peaks of HA samples with the increase of Hg(II) concentration was observed, and the experimental data agreed with the best-fitting line calculated based on the Ryan and Weber model. However, the relatively strong deviation of experimental

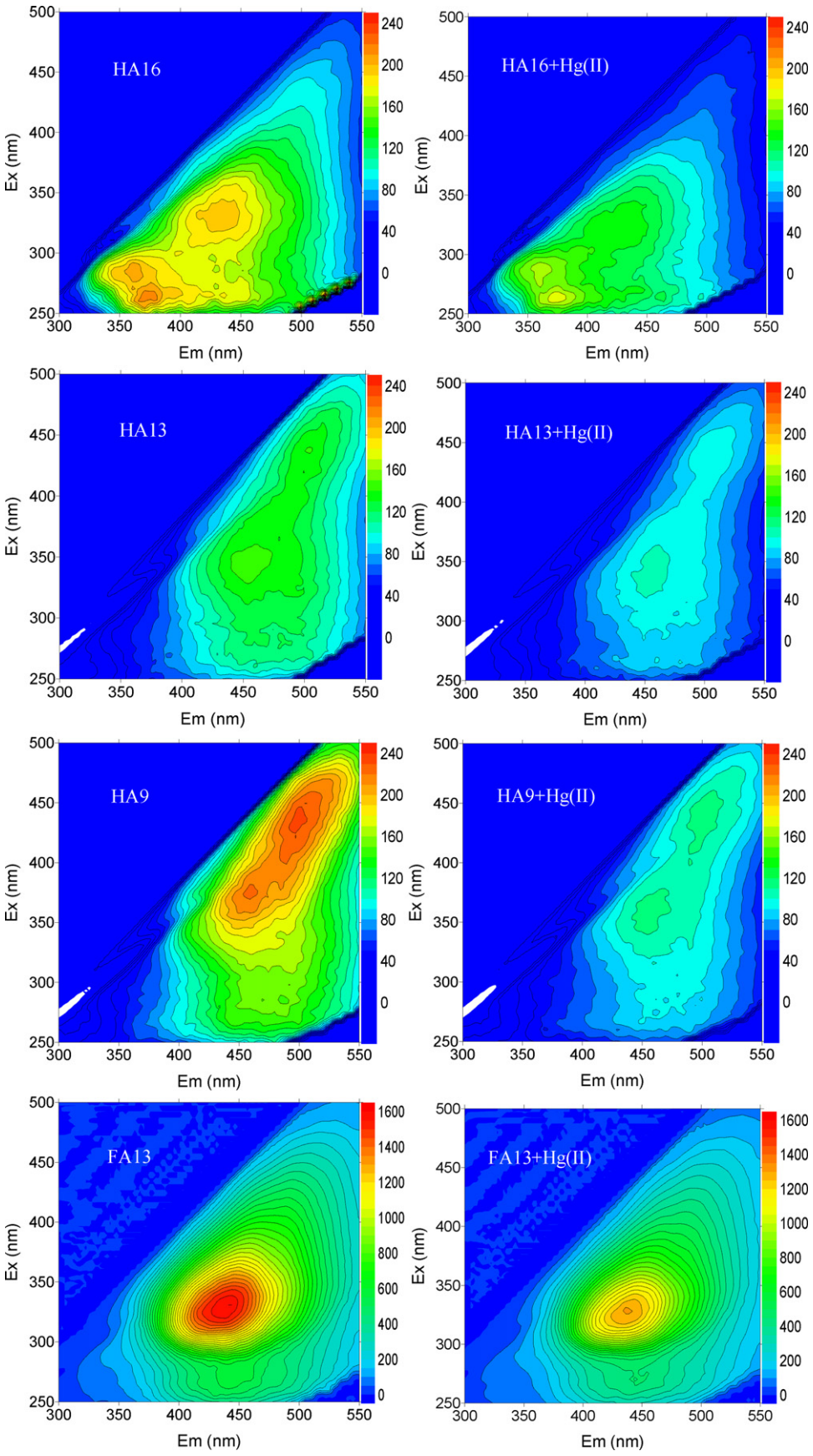

Fig. 2. The EEMs of HAs and FA in the absence and presence of Hg(II) at a total concentration of 30 μM.

data from the fitted curve and the slightly low values of r^2 of FA indicate that the quality of fitting for FA13 was not as good as for the HA samples.

FA13 is mainly composed of low-molecular-weight units of small aromatic condensation, high carboxylic groups, and other more easily oxidized substituents. So the binding sites for Hg(II) in FA are more complex than that in HA, which led to several fluorophore populations that are not equally accessible to the quencher of Hg(II) in the same fluorescence peak and thus deviation from the 1:1 stoichiometric in the Ryan and Weber model. This theory was further confirmed by fitting the fluorescence titration data using the modified Stern–Volmer model, which also assumes to form only 1:1 complexes between metal and ligand but takes into account the part of fluorescent sites that have no metal ion complexation properties. The experimental datasets of all the samples fit fairly well with the model except for that of FA13, which deviated from

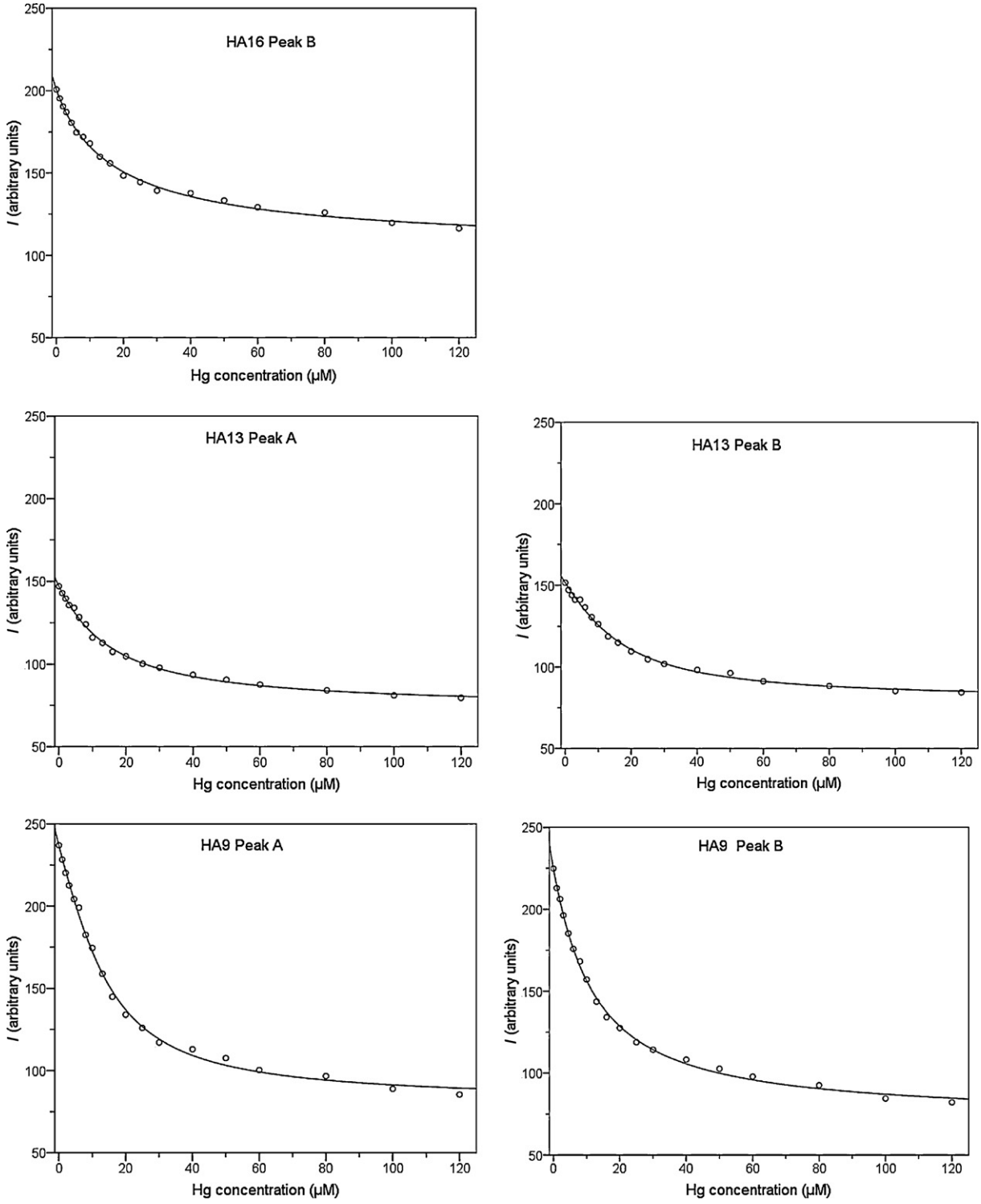

Fig. 3. Experimentally determined and model-derived non-linear regression of fluorescence intensity (I) of the main peaks detected in the EEMs of HAs and FA as a function of increasing total concentration (CM) of Hg(II) ion.

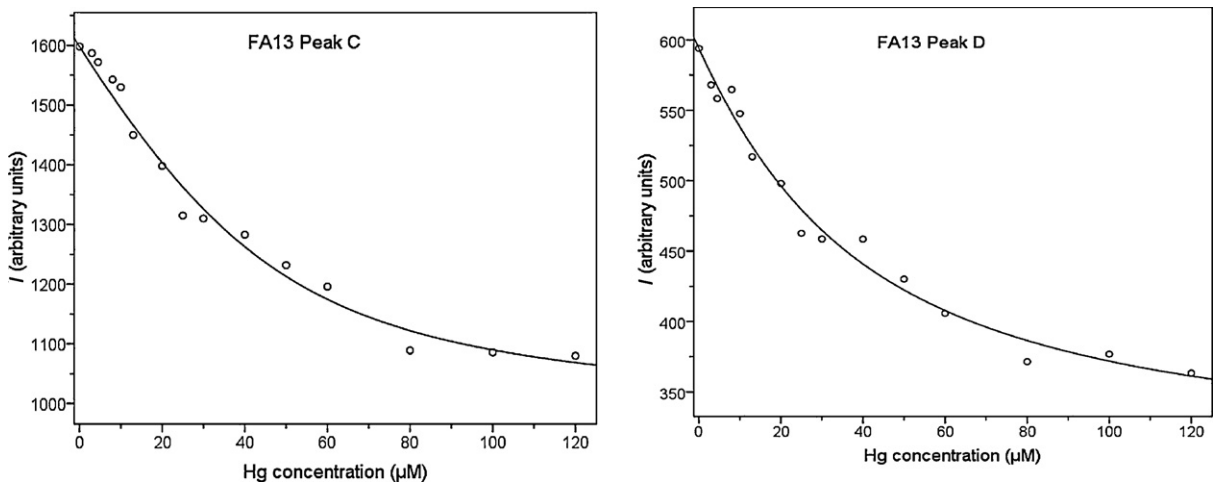

Fig. 3. (*Continued*).

linearity toward the *y*-axis for peak C (data not shown). This was in accordance with the results reported by Cook and Langford [30] that there are at least three fluorophore populations that behave differently in the binding process of Cu with the fluorescence peak of an FA.

According to Esteves da Silva et al. [31], there is a limitation with the non-linear Ryan and Weber model: a relatively high imprecision exists for the estimated C_L when the concentration of the binding sites or the conditional stability constants are relatively low. However, this constant has hardly any effect on other fitting parameters. As shown in Table 1, the negative C_L value determined for HA16 was just a reflection of the weakness of the model introduced by Ryan and Weber; the findings are consistent with the relatively small conditional stability constant for HA16 and demonstrate that the concentration of binding sites on HA16 may be very low. An attempt to estimate the three binding parameters using the non-linear Ryan and Weber model also led to negative C_L values for certain samples by other researchers such as Monteil-Rivera and Dumonceau [32] and Ryan and Weber [24].

As shown in Table 1, the stability constants of Hg(II)–HA complexes generally followed the order HA16 < HA13 < HA9. The Hg(II) ion complexing capacities of HA13 and HA9 were more or less the same though they were much higher than that of HA16. As determined in our previous study, S accounted for 1–2 mass% of total HS [25]. In the fluorescence quenching titration experiment, HS solution concentration was set at 50 mg/L and the Hg concentration was from 0 to 120 μmol/L. So the final Hg to S mol ratio in the reaction solution was as high as 4:1. Although Hg was expected to preferentially bind with thiol and other sulfur-containing groups, it mainly bound to the abundant oxygen functional groups other than sulfur groups because of the high Hg/S ratios adopted in the fluorescence quenching titration. As suggested by Ravichandran [33], the log *K* of Hg binding to S especially reduced S functional groups is generally higher than 10. The much lower overall stability constants of Hg with HS (4.5–5.2) further confirmed that oxygen-containing functional groups like carboxylic functional groups or phenolic groups, not the organic S especially reduced S groups, acted as the primary binding sites for Hg and governed the complexing behavior. The amount of elemental O and the number of carboxylic functional groups in HA decreased from HA9 to HA16 as landfill time increased, which created a decreasing trend for the stability constant of Hg(II)–HA complexes from HA9 to HA16 and the much lower Hg(II) complexing capacity of HA16 than that of HA9 or HA13. Furthermore, the aromatic condensation and humification degrees increased, so the hydrophobic property of HA increased from HA9 to HA16, which resulted in the smaller stability constant of HA as landfill time increased. It is well known that two adjacent aromatic carboxyl groups (i.e., a phthalic acid-like binding site) and an aromatic carboxyl group and adjacent phenolic OH group (i.e., a salicylic acid-like binding site) in the HA structure can form highly stable bidentate complexes with metal ions [19,20]. The decreasing trend of elemental O and carboxylic functional groups and the increasing trend of molecular structure size and molecular weight from HA9 to HA16 inevitably led to less of the strong phthalic acid-like and salicylic acid-like binding sites, which contributed to the decreasing of Hg(II)–HA complexes from HA9 to HA16. FA13 had a much higher Hg(II) complexing capacity compared to HA samples, which may be ascribed to its relatively high content of elemental O and carboxylic groups which was twice that of HA. FA is the part of HS that is not as mature as HA and would be degraded and changed into HA as landfill time increased. These results imply that FA played an important role in binding Hg(II) in early landfill stabilization processes.

Table 1
Fitting parameters of the non-linear Ryan–Weber model, i.e., fluorescence intensity of the Hg(II)–saturated HS complexes (I_{ML}), stability constant (log *K*) of Hg(II)–HS complexes, Hg(II) complexing capacity (C_L) of HS and the correlation coefficient for predicted and measured fluorescence intensity.

Parameter	HA16	HA13		HA9		FA13	
	Peak B	Peak A	Peak B	Peak A	Peak B	Peak C	Peak D
I_{ML}	105.2	73.1	78.9	80.1	72.2	979.2	298.0
log *K*	4.70	4.89	4.99	5.17	4.98	4.85	4.54
C_L	−0.077	0.100	0.248	0.255	0.063	0.863	0.348
r	0.997	0.997	0.997	0.997	0.998	0.984	0.982

3.4. Influence of pH on the complexation

Because pH influences the speciation of Hg(II), deprotonation of the functional groups of HS and the molecular conformation of HS [34–36], it is important to probe the fluorescence quenching titration of Hg(II) under various pH conditions. As shown in Fig. 4, aside from that of HA9, the fluorescence quenching efficiency of both peaks of the samples had similar trends as a function of pH. The maximum fluorescence quenching occurred at pH of 7.0 for HA16, 5.5–6.5 for HA13, and 6.5 for peak B of HA9; a constant fluorescence quenching efficiency was found between pH 6.5 and 9.0 for peak A of HA9. As for FA13, there were three peak values of fluorescence quenching efficiency, which occurred at pH 5.5–6.5, 7.5–8.5, and 9.5–10.5, respectively, with the maximum produced

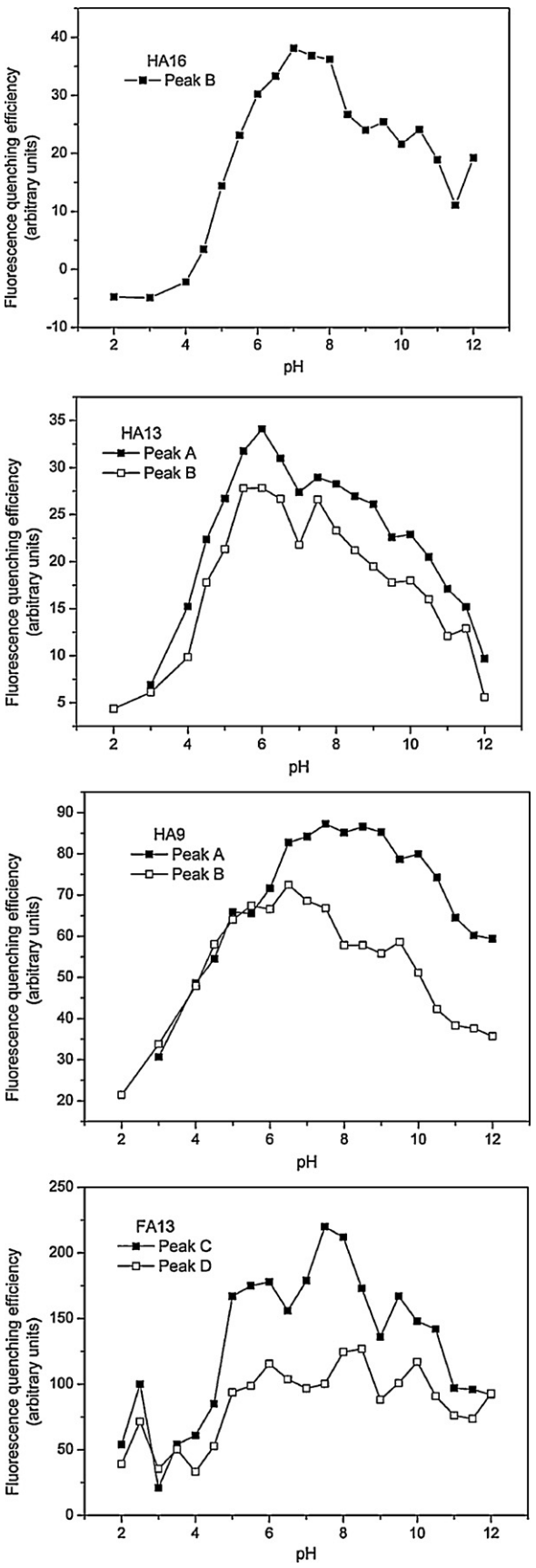

Fig. 4. The fluorescence quenching efficiency of HSs with 20 μM Hg(II) as a function of pH. The fluorescence quenching efficiency is calculated through the subtraction of the fluorescence intensity in the presence of 20 μM Hg(II) by that in the absence of 20 μM Hg (II).

at pH 7.5–8.5. This may correlate with the deprotonation of different functional groups at different pH ranges and thus different complexation properties of FA–Hg(II) complexes. The weak fluorescence quenching observed at a relatively strong acid condition was likely caused by the competition between protons and Hg(II) ions for the binding sites and the coiled structure of the HS molecules that prevented the access of Hg(II). Also, the hydrolysis of Hg(II), forming $Hg(OH)_2$, may have resulted in weak fluorescence quenching under relatively strong alkaline conditions. Strong fluorescence quenching at an approximately neutral pH condition is in accordance with previous studies [23,37]. The usually neutral pH value of a stabilized landfill suggests a great Hg(II) complexing capacity of HS and thus the relatively important role HS plays in the Hg(II) transformation in a stabilized landfill.

4. Conclusion

3DEEM fluorescence spectroscopy was used to investigate the complexing properties of HS from different landfill stabilization processes with Hg(II) ions. The fluorescence EEM spectra of the HS from different landfill stabilization processes when interacting with Hg(II) demonstrated the different interaction modes and the strength of the achieved bonding of Hg(II) to HS because of its functional chemical properties. The much lower overall stability constants of Hg with HA in this study suggest that oxygen-containing functional groups such as carboxylic functional or phenolic groups, other than organic S groups, act as the primary binding sites for Hg and govern complexing behavior.

The stability constant and complexing capacity of HA tended to decrease as landfill time extended. With HA as the main component of the stabilized landfill, the decrease of complexing capacity of HA with Hg(II) suggests that there was an increasing release of Hg from landfills as landfill time increased. FA exhibited a much higher Hg(II) complexing capacity than that of HA. FA, as the less matured or stabilized substance when compared to HA, would be degraded and changed into HA as landfill time increased. The findings imply that FA may play a more important role in binding Hg(II) in the early landfill stabilization process.

Acknowledgment

This work was supported by the National Natural Science Foundation of China (20877057, 51078285).

References

[1] S.E. Lindberg, J.L. Price, Airborne emissions of mercury from municipal landfill operations: a short-term measurement study in Florida, J. Air Waste Manag. Assoc. 49 (1999) 520–532.
[2] S.E. Lindberg, D. Wallschlager, E.M. Prestbo, N.S. Bloom, J. Price, D. Reinhart, Methylated mercury species in municipal waste landfill gas sampled in Florida, USA, Atmos. Environ. 35 (2001) 4011–4015.
[3] K.H. Kim, M.Y. Kim, G. Lee, The soil–air exchange characteristics of total gaseous mercury from a large-scale municipal landfill area, Atmos. Environ. 35 (2001) 3475–3493.
[4] K.H. Kim, M.Y. Kim, J. Kim, G. Lee, The concentrations and fluxes of total gaseous mercury in a western coastal area of Korea during late March 2001, Atmos. Environ. 36 (2006) 3413–3427.
[5] X.B. Feng, S.L. Tang, Z.G. Li, S.F. Wang, L. Liang, Landfill is an important atmospheric mercury emission source, Chin. Sci. Bull. 49 (2004) 2068–2072.
[6] X.B. Feng, G.H. Li, G.L. Qiu, A preliminary study on mercury contamination to the environment from artisanal zinc smelting using indigenous methods in Hezhang County, Guizhou, China. Part 2. Mercury contaminations to soil and crop, Sci. Total Environ. 368 (2006) 47–55.
[7] C.D.A. Earle, R.D. Rhue, J.F.K. Earle, Mercury in a municipal solid waste landfill, Waste Manag. Res. 17 (1999) 305–312.
[8] N.J. O'Driscoll, R.D. Evans, Analysis of methyl mercury binding to freshwater humic and fulvic acids by gel permeation chromatography/hydride generation ICP-MS, Environ. Sci. Technol. 34 (2000) 4039–4043.
[9] A.R. Khwaja, P.R. Bloom, P.L. Brezonik, Binding constants of divalent mercury (Hg^{2+}) in soil humic acids and soil organic matter, Environ. Sci. Technol. 40 (2006) 844–849.

[10] M. Haitzer, R.G. Aiken, N.J. Ryan, Binding of mercury(II) to aquatic humic substances: influence of pH and source of humic substances, Environ. Sci. Technol. 37 (2003) 2436–2441.
[11] F.C. Wu, Y.R. Cai, D. Evans, P. Dillon, Complexation between Hg(II) and dissolved organic matter in stream waters: an application of fluorescence spectroscopy, Biogeochemistry 71 (2004) 339–351.
[12] J.B. Shanley, P.F. Schuster, M.M. Reddy, D.A. Roth, H.E. Taylor, G.R. Aiken, Mercury on the move during snowmelt in Vermont, EOS 83 (2002) 45–48.
[13] R.K. Kolka, D.F. Grigal, E.S. Verry, E.A. Nater, Mercury and organic carbon relationships in streams draining forested upland/peatland watersheds, J. Environ. Qual. 28 (1999) 766–775.
[14] S.E. Lindberg, G. Southworth, E.M. Prestbo, D. Wallschlger, M.A. Bogle, J. Price, Gaseous methyl- and inorganic mercury in landfill gas from landfills in Florida, Minnesota, Delaware, and California, Atmos. Environ. 39 (2005) 249–258.
[15] S.M. Ullrich, T.W. Tanton, S.A. Abdrashitova, Mercury in the aquatic environment: a review of factors affecting methylation, Crit. Rev. Environ. Sci. Technol. 31 (2001) 241–293.
[16] R. Ebinghaus, H. Hintelmann, R.D. Wilken, Mercury-cycling in surface waters and in the atmosphere-species analysis for the investigation of transformation and transport-properties of mercury, Anal. Chem. 350 (1994) 21–29.
[17] R.D. Wilken, R. Falter, Determination of methylmercury by the species-specific isotope addition method using a newly developed HPLC–ICP MS coupling technique with ultrasonic nebulization, Appl. Organomet. Chem. 12 (1998) 551–557.
[18] N. Senesi, Metal–humic substance complexes in the environment. Molecular and mechanistic aspects by multiple spectroscopic approach, in: D.C. Adriano (Ed.), Biogeochemistry of Trace Metals, Lewis Publishers, Boca Raton, 1992, pp. 429–496.
[19] C. Plaza, G. Brunetti, N. Senesi, A. Polo, Molecular and quantitative analysis of metal ion binding to humic acids from sewage sludge and sludge-amended soils by fluorescence spectroscopy, Environ. Sci. Technol. 40 (2006) 917–923.
[20] C. Plaza, G. Brunetti, N. Senesi, A. Polo, Fluorescence characterization of metal ion, humic acid interactions in soils amended with composted municipal solid wastes, Anal. Bioanal. Chem. 386 (2006) 2133–2140.
[21] H. Diana, C. Plaza, N. Senesi, A. Polo, Detection of copper(II) and zinc(II) binding to humic acids from pig slurry and amended soils by fluorescence spectroscopy, Environ. Pollut. 143 (2006) 212–220.
[22] P.Q. Fu, F.C. Wu, C.Q. Liu, F.Y. Wang, W. Li, L.X. Yue, Q.J. Guo, Fluorescence characterization of dissolved organic matter in an urban river and its complexation with Hg(II), Appl. Geochem. 22 (2007) 1668–1679.
[23] D.Y. Zhang, X.L. Pan, K.M.G. Mostofa, X. Chen, G.J. Mu, F.C. Wu, J. Liu, W.J. Song, J.Y. Yang, Y.L. Liu, Q.L. Fu, Complexation between Hg(II) and biofilm extracellular polymeric substances: an application of fluorescence spectroscopy, J. Hazard. Mater. 175 (2010) 359–365.
[24] D.K. Ryan, J.H. Weber, Fluorescence quenching titration for determination of complexing capacities and stability constants of fulvic acid, Anal. Chem. 54 (1982) 986–990.
[25] X.L. Chai, G.X. Liu, X. Zhao, Y.C. Zhao, Composition and spectroscopic characteristics of humic substances in a landfill, J. Tongji Univ. 39 (2011) 392–396 (in Chinese).
[26] N. Senesi, T.M. Miano, M.R. Provenzano, G. Brunetti, Characterization, differentiation and classification of humic substances by fluorescence spectroscopy, Soil Sci. 152 (1991) 259–271.
[27] M.R. Silva, Estudospotenciomce spectroscfluorimospotenciomce spectroscopyon and classificada complexacão de metais com o Obisdien e as substis com o Obisdienyon and classificada complexacã substanc river and its complexation with Universidade Federal de Santa Catarina, 1996.
[28] W. Chen, P. Westerhoff, J.A. Leenheer, K. Booksh, Fluorescence excitation–emission matrix regional integration to quantify spectra for dissolved organic matter, Environ. Sci. Technol. 37 (2003) 5701–5710.
[29] T.M. Miano, G. Sposito, J.P. Martín, Fluorescence spectroscopy of humic substances, Soil Sci. Soc. Am. J. 52 (1988) 1016–1019.
[30] R.L. Cook, C.H. Langford, Metal ion quenching of fulvic acid fluorescence intensities and lifetimes: nonlinearities and a possible three-component model, Anal. Chem. 67 (1995) 174–180.
[31] J.C.G. Esteves da Silva, A.A.S.C. Machado, C.J.S. Oliveira, M.S.S.D.S. Pinto, Fluorescence quenching of anthropogenic fulvic acids by Cu(II), Fe(III) and UO_2^{2+}, Talanta 45 (1998) 1155–1165.
[32] F. Monteil-Rivera, J. Dumonceau, Fluorescence spectrometry for quantitative characterization of cobalt(II) complexation by leonardite humic acid, Anal. Bioanal. Chem. 374 (2002) 1105–1112.
[33] M. Ravichandran, Interactions between mercury and dissolved organic matter—a review, Chemosphere 55 (2004) 319–331.
[34] J. Luster, T. Lloyd, G. Sposito, Multi-wavelength molecular fluorescence spectrometry for quantitative characterization of copper(II) and aluminum(III) complexation by dissolved organic matter, Environ. Sci. Technol. 30 (1996) 1565–1574.
[35] K.K. Au, A.C. Penisson, S.L. Yang, C.R. O'Melia, Natural organic matter at oxide/water interfaces: complexation and conformation, Geochim. Cosmochim. Acta 63 (1999) 2903–2917.
[36] N. Patel-Sorrentino, S. Mounier, J.Y. Benaim, Excitation–emission fluorescence matrix to study pH influence on organic matter fluorescence in the Amazon basin rivers, Water Res. 36 (2002) 2371–2581.
[37] X.Q. Lu, R. Jaffe, Interaction between Hg(II) and natural dissolved organic matter: a fluorescence spectroscopy based study, Water Res. 35 (2001) 1793–1803.